

Microstructure and optical properties of free-standing porous silicon films: Size dependence of absorption spectra in Si nanometer-sized crystallites

Yoshihiko Kanemitsu, Hiroshi Uto, and Yasuaki Masumoto
Institute of Physics, University of Tsukuba, Tsukuba, Ibaraki 305, Japan

Takahiro Matsumoto, Toshiro Futagi, and Hidenori Mimura
Electronics Research Laboratories, Nippon Steel Corporation, Sagami-hara, Kanagawa 229, Japan

(Received 30 March 1993; revised manuscript received 1 June 1993)

We have studied the microstructure and optical properties of free-standing porous Si thin films fabricated by electrochemical anodization. Raman-spectroscopy and transmission-electron-microscopy examinations show that Si crystallite spheres with diameters of several nanometers are dispersed in the amorphous phase. The blueshift of the optical-absorption spectrum is observed for decreasing average diameter of the Si crystallites. However, there is no clear size dependence of the peak energy of the broad photoluminescence (PL) spectrum. Spectroscopic analysis strongly suggests that the photogeneration of carriers occurs in the *c*-Si core, whose band gap is modified by the quantum-confinement effect, while the strong PL comes from the near-surface region of small crystallites.

Very recently, many attempts have been made to produce quasi-direct-gap semiconductor nanostructures made from indirect-gap semiconductors and a great deal of research effort¹⁻⁵ is focused on nanometer-size crystallites or quantum dots made from Si or Ge. Strong photoluminescence (PL) from Si nanostructures fabricated by electrochemical anodization, often called porous Si, has attracted much attention from a fundamental-physics viewpoint and because of the potential application to optical devices. However, despite many attempts to determine the origin of the strong PL, the origin and mechanism of visible PL in porous Si are not understood yet and several models have been suggested. One model is that the quantum-confinement effect in Si nanocrystallites enhances the oscillator strength of the direct optical transitions and gives efficient radiation from porous Si.⁶⁻⁹ On the other hand, with a large surface-to-volume ratio in the highly porous structure, surface localized states in Si nanocrystallites are considered to be responsible for the origin of luminescence of porous Si.¹⁰⁻¹² Moreover, silicon-based compounds such as siloxene (Si₆O₃H₆) derivatives¹³ or the rearranged Si-Si bonds like small H-terminated Si clusters¹⁴ formed at the surface are also proposed as an origin of the strong PL of porous Si.

To discuss the quantum-confinement effect on electronic processes in nanocrystallites, we need to know the size dependence of both optical absorption and PL properties of nanocrystallites. The blueshift of absorption spectra due to the quantum-confinement effect is observed in a variety of semiconductor nanocrystallites; however, we have no information about the size dependence of the optical-absorption spectrum in porous Si. It is important to identify the optical-absorption process and compare absorption spectra with PL spectra in porous Si.

In this paper we have studied optical absorption and PL spectra of free-standing porous Si films. We observed that the blueshift of the optical-absorption spectrum of

porous Si occurs with a decrease in the average diameter of Si crystallites. The PL spectrum scarcely depends on the size of Si crystallite. These results strongly suggest that the photogeneration of carriers occurs in the crystalline Si (*c*-Si) core with the band gap modified by the quantum-confinement effect, while the visible room-temperature PL comes from the near-surface region of crystallites.

The free-standing porous silicon layers were prepared as described in the literature.¹⁵ The substrates were (100)-oriented *p*-type silicon wafers with resistivities of 0.2, 3.5, 10, 50, and 230 Ω cm. Thin Al films were evaporated on the back of the wafers to form a good Ohmic contact. The anodization was carried out in HF-ethanol solution (HF:H₂O:C₂H₅OH = 1:1:2) at a constant current density of 30 mA/cm² for 15–60 min. After the anodization, we abruptly increased the current density up to about 700 mA/cm² and electrochemically removed the porous Si layer from the Si substrate. The porous silicon films were finally rinsed in C₂H₅OH solution. The thickness of porous Si films was 20–40 μm.

Microstructures of these porous Si films were studied using TEM analysis and Raman spectroscopy. TEM microscopy was performed using a JEOL 2010 system operated at 200 keV. Raman-scattering measurements were performed at room temperature in a backscattering configuration. Raman spectra were obtained using 514.5-nm laser light and a Raman microprobe measurement system (Japan Spectroscopic Co. Ltd., R-MPS-11) consisting of a 25-cm filter monochromator and a 1-m monochromator. The PL spectra of porous Si films were measured in a vacuum by using 325-nm excitation light from a He-Cd laser. The calibration of the spectral sensitivity of the whole measuring system was performed by using a tungsten standard lamp. The optical-absorption spectra were measured using a spectrometer with an integrating sphere (Hitachi Ltd., U-4000) in order to reduce

the effects of light scattering from porous Si. Spectroscopic data were measured at room temperature.

Figure 1 shows a typical TEM image of local structure of a porous Si film prepared from the 3.5- Ω cm wafer. Porous silicon is a mixture of Si crystallite spheres and an amorphous phase. Our TEM observations of free-standing porous Si films are similar to those of porous Si layers reported previously.¹⁶ Si crystallite spheres with various diameters are observed and the typical diameter of Si crystallite spheres is several nanometers. These structures are also confirmed with Raman spectroscopy. The average diameter of Si crystallites is determined from Raman spectra, as shown below.

Figure 2 shows Raman spectra of free-standing porous Si films. Broad and downshift signals were observed in porous Si, as compared with those of *c*-Si bulk. Here, we shall evaluate the average diameter of Si crystallite spheres, L , using a spatial correlation model.^{17,18} Finite-size effects relax the q -vector selection rule and this relaxation of the momentum conservation leads to a downshift and broadening of the Raman spectrum.¹⁷ A quantitative model (strong phonon confinement model with a phonon amplitude of ~ 0 at the boundary)¹⁸ is usually used for the estimate of the average diameter of nanocrystals such as Si (Refs. 18 and 19) or Ge.²⁰ Hence we use the strong confinement model to determine the crystallite size in porous Si films. In this model, the first-order Raman spectrum $I(\omega)$ is given by¹⁸

$$I(\omega) = \int_0^1 \frac{\exp(-q^2 L^2 / 4a^2)}{[\omega - \omega(q)]^2 + (\Gamma_0/2)^2} d^3q, \quad (1)$$

where q is expressed in units of $2\pi/a$, a is the lattice constant, and Γ_0 is the linewidth of the Si LO phonon in *c*-Si bulk (~ 3.6 cm^{-1} including instrument contributions). We consider the dispersion $\omega(q)$ of the LO phonon in *c*-Si to be²¹

$$\omega^2(q) = A + B \cos(\pi q / 2), \quad (2)$$

where $A = 1.714 \times 10^5$ cm^{-2} and $B = 1.000 \times 10^5$ cm^{-2}

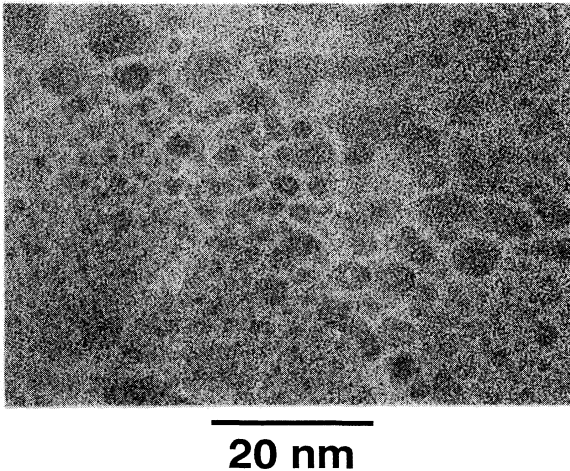


FIG. 1. TEM image of a free-standing porous Si film.

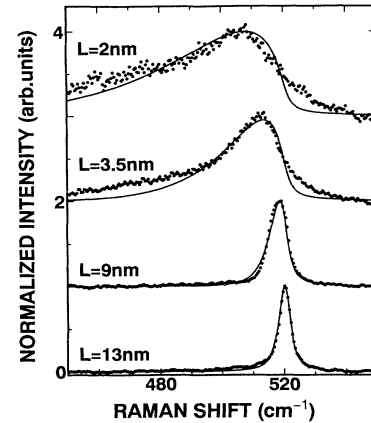


FIG. 2. Raman spectra of free-standing porous Si films compared with the spectra calculated for a sphere with diameter L (solid lines). The calculated spectra agree well with experimental ones.

These parameters were determined to describe the neutron scattering data clearly.²¹ By using Eqs. (1) and (2), we can calculate the Raman spectrum of nanocrystallites and estimate the average diameter of Si crystallites. Solid lines in Fig. 2 are calculated spectra, which agree well with the experimental results. Figure 3 summarizes the relationship between the Raman width and the Raman shift with respect to *c*-Si. The solid line indicates the theoretical calculations for spherical crystallites, and the experimental relationship between the Raman width and peak shift seems to be approximately consistent with calculations.²² The average diameter of crystallite spheres ranges from ~ 2 to ~ 10 nm. The average diameter calculated using the phonon confinement model is supported by TEM observations.

Typical optical absorption and PL spectra of porous Si films with different crystallite sizes [(a) $L \sim 2$ nm, (b) $L \sim 3.5$ nm, and (c) $L \sim 9$ nm] are shown in Fig. 4. A gradual increase in the optical-absorption coefficient α is observed near the absorption edge and at higher energies α monotonically increases. It is found that the blueshift

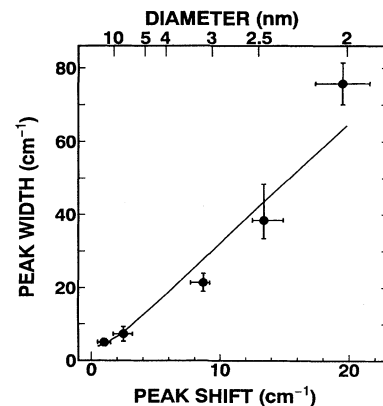


FIG. 3. The calculated relationship between the Raman width, the decrease of the Raman peak shift with respect to *c*-Si. L is the average diameter of Si crystallites.

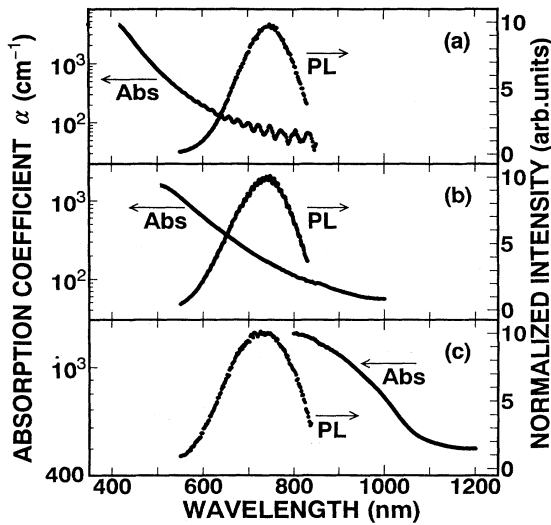


FIG. 4. Typical optical-absorption and photoluminescence spectra of porous Si films: (a) $L \sim 2$ nm, (b) $L \sim 3.5$ nm, and (c) $L \sim 9$ nm.

of optical-absorption spectrum occurs with a decrease in the average diameter of Si crystallites. In Fig. 4, no correction was made for the porosity of the sample films, p .^{1,2} If we consider the porosity and the optical density of the samples, it is reliable to use the optical-absorption edge as a value of the photon energy at $\alpha \geq 4 \times 10^2$ cm^{-1} .²³ Accordingly, for the present we define the optical band gap E_α as the photon energy at $\alpha = 6 \times 10^2$ cm^{-1} . The size dependence of E_α is shown in Fig. 5. The solid line shows the exciton energy in Si crystallite spheres calculated using an effective-mass approximation.⁹ The blueshift of the absorption edge strongly suggests that the quantum-confinement effect plays a key role in the absorption process. However, further investigations are needed both from theoretical and experimental points of view to clarify the relation between the band-gap energy and the diameter.

Figure 4 also shows the PL spectra of these films with different crystallite sizes. No significant size dependence of the PL peak energy was observed. The PL peak energy in samples with small average diameters [see Figs. 4(a)

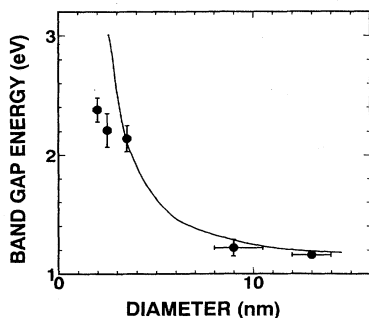


FIG. 5. Band-gap energy as a function of the diameter of crystalline Si spheres. The solid line is a theoretical calculation by an effective-mass approximation (Ref. 9).

and 4(b)] is much lower than the band gaps determined from both the experiment E_α and the theoretical calculations (see Fig. 5). The above PL characteristics and the blueshift of the absorption spectrum imply that the site for the photogeneration of carriers are different from that for radiative recombination of carriers. Moreover, in porous Si films having large Si crystallites, there appears an unusual relationship between the absorption and PL spectra: As shown in Fig. 4(c), the PL peak energy is higher than the absorption edge energy. In porous Si samples with large crystallite diameter, the PL excitation spectrum entirely differs from the optical-absorption spectrum. The shape of PL excitation spectrum in porous Si of $L \sim 9$ nm is similar to that of the absorption spectrum shown in Fig. 4(a). TEM studies also show that there are Si crystallites of various sizes in the sample. Thus, the unusual spectroscopic relation in Fig. 4(c) strongly suggests that only small crystallites contribute to the efficient visible PL.

Considering that the surface of Si nanocrystallites in porous Si is terminated by H atoms or OH groups,^{10,11,13,24} we believe that the electronic properties of the near-surface region are different from those of the *c*-Si core. To explain the size-dependent absorption and the size-independent PL spectra, we propose a simple model that the photogeneration of carriers occurs in the *c*-Si core whose band gap is modified by the quantum-confinement effect, whereas the radiative recombination occurs in the near-surface region.²⁵ In our model, the PL efficiency in the near-surface region increases with a decrease in the crystallite size, because both the surface-to-volume ratio and the carrier transfer rate from the core to the surface increase with a decrease in the size of crystallites.

The temperature dependence of the PL intensity also supports the above model. Figure 6 shows the temperature dependence of the PL intensity at 750 nm. In all sample films, the PL intensity increases with raising temperature up to about 100 K and then decreases. According to our model, this behavior is explained as follows: At low temperature, the carriers are generated in the core and some of the carriers in the *c*-Si core transfer to the near-surface region by a thermally activated diffusion process. At high temperature, the nonradiative recombination in the near-surface region increases and then the

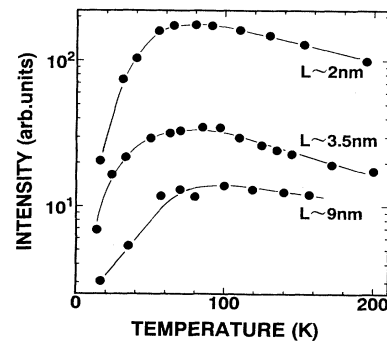


FIG. 6. Temperature dependence of the PL intensity in porous Si films of $L \sim 2$, ~ 3.5 , and ~ 9 nm. The PL intensity increases with raising the temperature up to about 100 K and then decreases gradually.

PL intensity decreases gradually. The PL efficiency is determined by both the thermal carrier-diffusion process from the *c*-Si core to the near-surface region and the radiative recombination rate in the near-surface region.

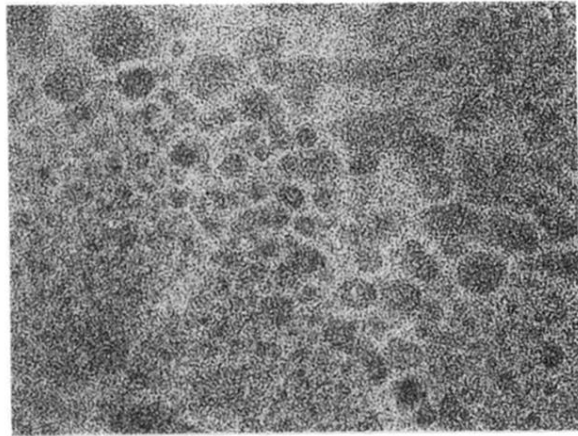
The above experimental facts (the size-dependent optical-absorption spectrum, the size-independent PL spectrum, the temperature dependence of the PL intensity, and the unusual spectroscopic relation in porous Si with the large average diameter of crystallites) can be explained by a simple picture: The photogeneration of carriers occurs in the *c*-Si core with the size-dependent band gap, and the radiative recombination in the near-surface region causes the strong visible PL at room temperature. The strong PL comes from the near-surface region of crystallites with sizes less than a certain diameter. Further theoretical and experimental studies are needed to

clarify the electronic structures of the luminescent near-surface region.

In conclusion, we studied the size dependence of the optical properties of free-standing porous Si films. It was found that the blueshift of the optical-absorption spectrum occurs with a decrease in the crystallite size. The electronic structure of porous Si is modified by the quantum-confinement effect. The near-surface region in small crystallites plays the most essential role in the visible PL processes of porous Si.

The authors would like to thank A. Yamamoto, T. Ogawa, K. Shiraishi, and K. Takeda for discussions. Part of this work was done at the Cryogenic Center, University of Tsukuba. One of the authors (Y.K.) is grateful to NISSAN Science Foundation for financial support.

- ¹L. T. Canham, *Appl. Phys. Lett.* **57**, 1046 (1990); A. G. Cullis and L. T. Canham, *Nature* **353**, 335 (1991).
- ²V. Lehmann and U. Gosele, *Appl. Phys. Lett.* **58**, 856 (1991).
- ³*Light Emission from Silicon*, edited by S. S. Iyer, R. T. Collins, and L. T. Canham, MRS Symposia Proceedings No. 256 (Materials Research Society, Pittsburgh, 1992).
- ⁴*Microcrystalline Semiconductors: Materials Science and Devices*, edited by P. M. Fauchet, C. C. Tsai, L. T. Canham, I. Shimizu, and Y. Aoyagi, MRS Symposia Proceedings No. 283 (Materials Research Society, Pittsburgh, 1993).
- ⁵Y. Kanemitsu *et al.*, *Appl. Phys. Lett.* **61**, 2178 (1992).
- ⁶S. Gardelis *et al.*, *Appl. Phys. Lett.* **59**, 2118 (1991).
- ⁷R. Tsu, H. Shen, and M. Dutta, *Appl. Phys. Lett.* **60**, 112 (1992).
- ⁸T. Ohno, K. Shiraishi, and T. Ogawa, *Phys. Rev. Lett.* **69**, 2400 (1992); A. J. Read *et al.*, *ibid.* **69**, 1232 (1992); F. Buda, J. Kohanoff, and M. Parinello, *ibid.* **69**, 1272 (1992).
- ⁹T. Takagahara and K. Takeda, *Phys. Rev. B* **46**, 15 578 (1992).
- ¹⁰M. A. Tischler, R. T. Collins, J. H. Stathis, and J. C. Tsang, *Appl. Phys. Lett.* **60**, 639 (1992); J. C. Tsang, M. A. Tischler, and R. T. Collins, *ibid.* **60**, 2279 (1992).
- ¹¹C. Tsai *et al.*, *Appl. Phys. Lett.* **60**, 1700 (1992).
- ¹²T. George *et al.*, *Appl. Phys. Lett.* **60**, 2359 (1992).
- ¹³M. S. Brandt *et al.*, *Solid State Commun.* **81**, 307 (1992); P. Deak *et al.*, *Phys. Rev. Lett.* **69**, 2531 (1992).
- ¹⁴Y. Kanemitsu *et al.*, *Appl. Phys. Lett.* **61**, 2446 (1992).
- ¹⁵H. Koyama *et al.*, *Jpn. J. Appl. Phys.* **30**, 3606 (1991); N. Koshida and H. Koyama, in *Light Emission from Silicon* (Ref. 3), p. 219.
- ¹⁶M. W. Cole *et al.*, *Appl. Phys. Lett.* **60**, 2800 (1992); Y. Kanemitsu, T. Matsumoto, T. Futagi, and H. Mimura, in *Microcrystalline Semiconductors: Materials Science and Devices* (Ref. 4), p. 221.
- ¹⁷H. Richter, Z. P. Wang, and L. Ley, *Solid State Commun.* **39**, 625 (1981).
- ¹⁸I. H. Campbell and P. M. Fauchet, *Solid State Commun.* **58**, 739 (1984).
- ¹⁹Z. Sui, P. P. Leong, I. P. Herman, G. S. Higashi, and H. Temkin, *Appl. Phys. Lett.* **60**, 2086 (1992).
- ²⁰M. Fujii, S. Hayashi, and K. Yamamoto, *Appl. Phys. Lett.* **57**, 2692 (1990).
- ²¹R. Tubino, L. Piseri, and G. Zerbi, *J. Chem. Phys.* **56**, 1022 (1972).
- ²²For small crystallites, there is a difference between the experimental and theoretical results. In the theoretical calculation, we consider that the crystallites are spherical. However, TEM studies (Ref. 1) show that there exist cylindrically shaped crystallites as well as spherical crystallites in porous Si. Our results suggest that in small crystallites, the Raman spectra are sensitive to the shape of the crystallites and a more detailed calculation of Raman spectra should take into account the various shapes of crystallites.
- ²³If we assume that the number of photons absorbed in the sample film depends on the porosity p and is proportional to $(1-p)$, the corrected optical absorption coefficient β is approximately given by $\beta = \alpha - [\ln(1-p)]/d$, where α is the absorption coefficient of the sample film determined from the transmission spectrum without the correction of porosity and d is the sample thickness. Using values of $p \sim 0.6-0.8$ (e.g., Refs. 1 and 2) and $d \sim 40 \mu\text{m}$, the correction term of $-[\ln(1-p)]/d$ is estimated to be $\sim 2-4 \times 10^2 \text{ cm}^{-1}$, which is independent of the wavelength.
- ²⁴T. Masumoto, T. Futagi, H. Mimura, and Y. Kanemitsu, *Phys. Rev. B* **47**, 13 879 (1993).
- ²⁵We consider that the radiative recombination efficiency in the Si core is very low, because the electronic properties of the *c*-Si core with diameters more than several nanometers show the indirect-gap nature like the bulk Si (in Ref. 9) and the optical transition strength is small due to the indirect character; Y. Kanemitsu, T. Ogawa, K. Shiraishi, and K. Takeda, *Phys. Rev. B* (to be published).



20 nm

FIG. 1. TEM image of a free-standing porous Si film.